

Article

Seismic Fragility Evaluation of Main Steam Piping of Isolated APR1400 NPP Considering the Actual Failure Mode

Bub-Gyu Jeon ¹, Sung-Wan Kim ^{1,*}, Da-Woon Yun ¹, Daegi Hahm ² and Seunghyun Eem ^{3,*}

¹ Seismic Research and Test Center, Pusan National University, Yangsan-si 50612, Korea; bkjeon79@pusan.ac.kr (B.-G.J.); ardw818@pusan.ac.kr (D.-W.Y.)

² Advanced Structures and Seismic Safety Research Division, Korea Atomic Energy Research Institute, Daejeon 37224, Korea; dhahm@kaeri.re.kr

³ Department of Convergence & Fusion System Engineering, Kyungpook National University, Sangju 41566, Korea

* Correspondence: swkim09@pusan.ac.kr (S.-W.K.); eemsh@knu.ac.kr (S.E.)

Abstract: An isolation system installed in a nuclear power plant (NPP) could increase seismic safety during seismic events. On the other hand, a more significant relative displacement may occur due to the isolation system. The seismic risk could be increased in the case of an interface piping system that connects isolated and nonisolated structures. Therefore, it is necessary to consider the piping systems when evaluating the safety of isolated-NPPs. This study performed seismic fragility analysis with isolated APR1400 nuclear power plants with the main steam piping. The main steam piping is the interface pipe connecting the isolated auxiliary building and the turbine building. The failure mode for seismic fragility analysis was defined as cracks caused by leakage. The experimental and numerical analysis results quantified the leak-through crack point as a damage index. The seismic fragility curves are suggested based on peak ground acceleration and the relative displacement between the isolated and nonisolated buildings.

Keywords: base isolation; interface pipe; fragility analysis; seismic performance



Citation: Jeon, B.-G.; Kim, S.-W.; Yun, D.-W.; Hahm, D.; Eem, S. Seismic Fragility Evaluation of Main Steam Piping of Isolated APR1400 NPP Considering the Actual Failure Mode. *Sustainability* **2022**, *14*, 8315. <https://doi.org/10.3390/su14148315>

Academic Editor: Maged A. Youssef

Received: 18 May 2022

Accepted: 30 June 2022

Published: 7 July 2022

Publisher's Note: MDPI stays neutral with regard to jurisdictional claims in published maps and institutional affiliations.



Copyright: © 2022 by the authors. Licensee MDPI, Basel, Switzerland. This article is an open access article distributed under the terms and conditions of the Creative Commons Attribution (CC BY) license (<https://creativecommons.org/licenses/by/4.0/>).

1. Introduction

Seismic events can cause severe damage to a nuclear power plant (NPP). Therefore, the seismic safety of NPPs must be guaranteed. Isolation systems are widely used to secure the seismic safety of infrastructure, such as bridges and buildings. France introduced isolation systems in the 1980s to secure the seismic safety of NPPs, and they have been operating commercially in NPPs, such as Koeberg NPP and Cruas NPP. In Japan, after the Fukushima NPP incident, ongoing research is being conducted to install isolation systems in NPPs, and performance evaluation tests and seismic fragility analyses of the full-scale isolation system have been conducted. The United States conducted research to prepare guidelines related to isolation systems. Studies have also been conducted in Korea to evaluate the mechanical properties of isolation systems to considering the install them in NPPs [1].

The application of an isolation system can improve the seismic safety of NPPs, but the relative displacement between the isolated and nonisolated structures will be increased significantly. Therefore, the safety of some facilities due to the increased relative displacement must be evaluated. In particular, the crossover piping system that connects isolated and nonisolated structures must be able to encounter large relative displacements [2–4].

Research on the safety of crossover piping systems has been conducted. Shaking table tests [5] and seismic response analyses were performed to evaluate the seismic safety of the crossover piping system. They confirmed that the crossover piping system has a significantly larger relative displacement compared to the case of a general piping system. Therefore, the stress responses of the crossover piping system could exceed the allowable stress during ground motions that are dominant with long-period components [6]. Leakage

due to cracks in NPP piping is the actual failure that could cause serious accidents. Therefore, an experimental study was conducted to express the leakage of the pipe under seismic loads. The elbow is a representative seismic vulnerability component. Cyclic loading tests were performed for the estimation of the seismic capacity of piping elbows. At this time, the nonlinear behavior of the elbow and the damage index analysis based on low-cycle fatigue (LCF) were performed [7,8]. In addition, seismic fragility analysis of the crossover piping system was performed based on the damage index, which can represent leak-through cracks as a failure criterion [9]. Furthermore, seismic fragility analysis of the crossover piping system was performed using NRC-BNL benchmark model no. 4 [10]. On the other hand, this model was briefly applied to the design of nuclear power plants. Moreover, it is difficult to represent structures and piping systems with complex support conditions and shapes, which are different in Korean nuclear power plants. A simplified model was selected to prove the proposed methodology. A simplified seismic fragility analysis was performed for input ground motion considering the unidirectional (horizontal).

This study examined APR1400 (Advanced Power Reactor 1400), which is a representative Korean standard NPP. A nonlinear isolation system was applied to the lower part of the nuclear island. A finite element analysis was prepared for the main steam engine. A representative pipe connecting the isolated and nonisolated structures was evaluated, and seismic fragility analysis was performed. Thirty sets of input ground motion (bi-directional) were considered. Leak-through cracks, which are actual failures that can cause serviceability issues and serious accidents in the piping system, were defined as the failure modes. The damage index for leak-through cracks was used as a failure criterion for seismic fragility analysis. The seismic intensity of the seismic fragility curve used the peak ground acceleration (PGA) and MRD (relative displacement between the ground and the isolated floor).

2. Main Steam Piping of Isolated APR1400 NPP

The relative displacement could damage the crossover piping system that connects isolated and nonisolated structures. Therefore, a seismic response analysis of the isolated structure and relative displacement was conducted. The seismic responses of the isolated structure are dominated by isolative behavior. Therefore, an upper structure was simplified to a point-mass with two degrees of freedom in two directions (x , y). Seismic response analyses were performed using the Opensees program [11].

The target NPP was APR1400 [12,13], a Korean standard NPP. Figure 1 presents the concept of the APR1400 nuclear power plant with an isolation system. The isolation system was applied to a nuclear island, which is the foundation of the containment and auxiliary buildings. The upper structure, including the nuclear island, weighs 464,500 tons, and its size is 140 m \times 103 m [14]. The isolation system was assumed to have bilinear characteristics, as shown in Figure 2, and it was designed with reference to ASCE 7 [15] and FEMA451 [16]. The isolation system had an effective period of 2.5 sec and a damping ratio of 20% for a PGA of 0.5 g as the design levels. Table 1 lists the parameters for the isolation system.

Table 1. Parameters for the isolation system.

Parameters	Values
K_{eff}	2939.72 MN/m
K_u	19,620.51 MN/m
K_d	1962.05 MN/m
Q_d	329.43 MN

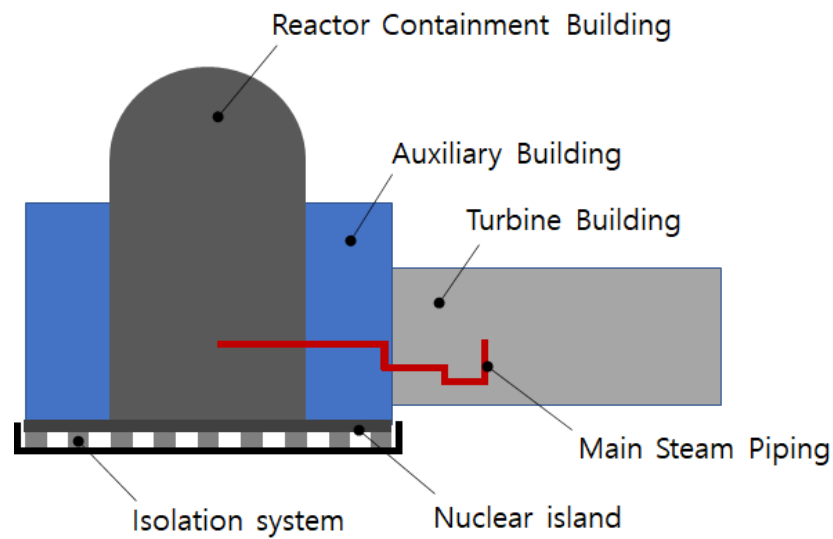


Figure 1. Concept of base-isolated APR 1400 [12,13].

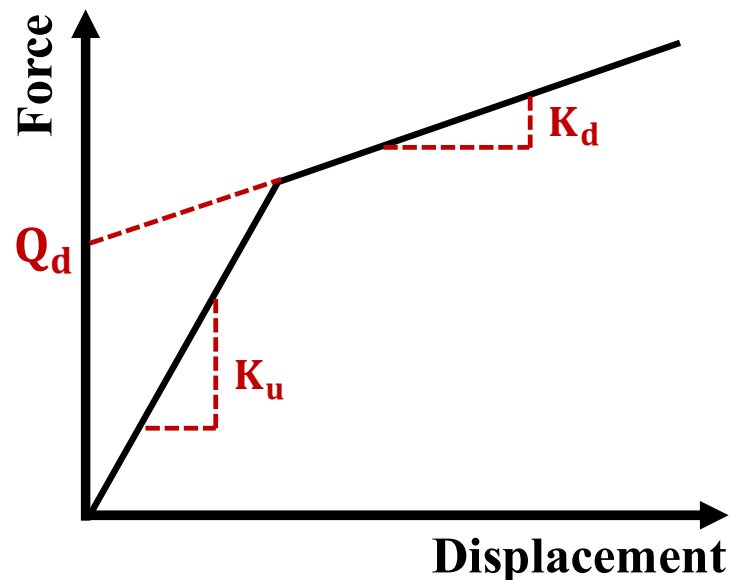


Figure 2. Mechanical properties of the isolation system.

Input earthquakes were modified to satisfy the response spectrum of Reg. Guide 1.60 [17] using the RSPmatch program, with the seismic records provided by the Pacific Earthquake Engineering Research Center (PEER). The input earthquake was composed of 30 sets from EQ1 to EQ30 in horizontal bidirections (x , y) and artificial earthquakes were generated in units of 0.5 g from 1.0 g to 3.0 g with the PGA level. The response spectrum is represented by a geometric mean. Hence, the directional uncertainty was applied by referring to ASCE4 [18]. Figure 3 shows a response spectrum for each direction of the generated input earthquake. The time history of the relative displacement between the isolated structure and the ground was derived by performing a seismic response analysis using the Opensees program for the target structure and the input earthquake. The PGA of the Great East Japan Earthquake was approximately 2.75 g, and the maximum ground acceleration measured in Shiogama, Hitachi, and Sendai also exceeded 1.53 g [19].

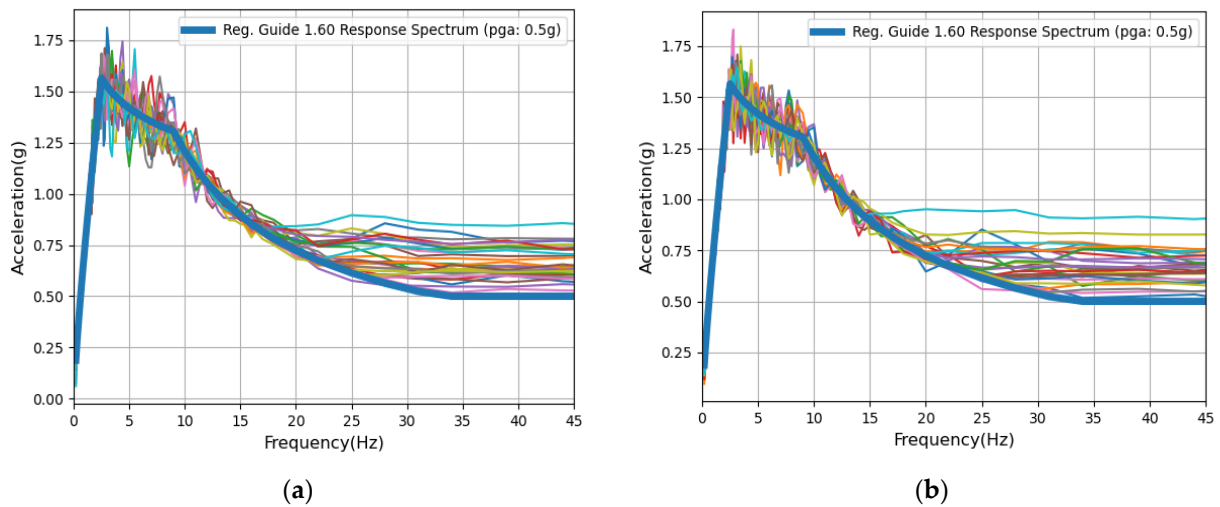


Figure 3. Response spectrum [13,14]: (a) x-directional; (b) y-directional.

In this study, the crossover piping system is the main steam piping with multiple supported and arranged by an auxiliary building on the isolated APR1400 NPP nuclear island and a turbine building, which is a nonisolated structure. A finite element model of the piping system was modeled using ABAQUS 6.14. Figure 4 and Table 2 present the main steam piping and its specifications, respectively.

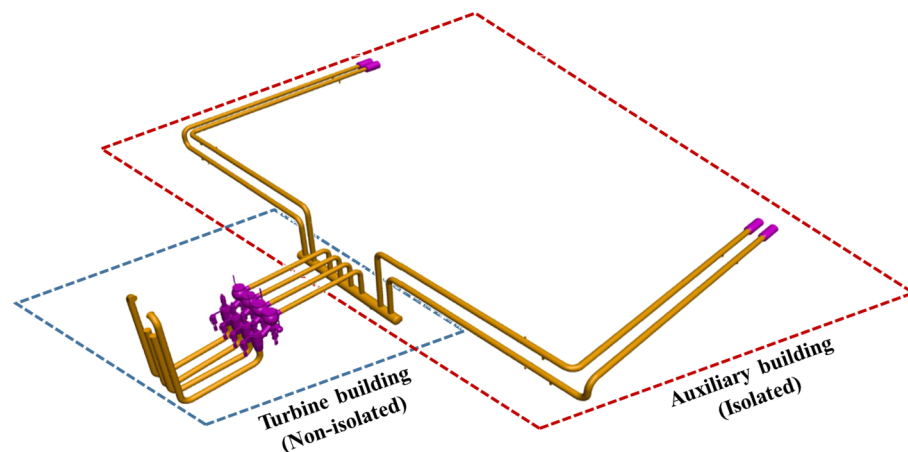


Figure 4. Main steam piping of isolated APR 1400.

Table 2. Specifications of the piping system.

Location	D [mm]	t [mm]	D/t
Turbine building	705.79	27.00	26.14
Auxiliary building	764.72	38.10	20.07
	1458.11	59.54	24.49

The material was assumed to be carbon steel SA106 and Grade B [20] of ASME B36.10M, which are commonly used in NPPs. The nonlinear material properties were derived from the material tensile test and defined as a bilinear type, as shown in Figure 5 and Table 3 [21].

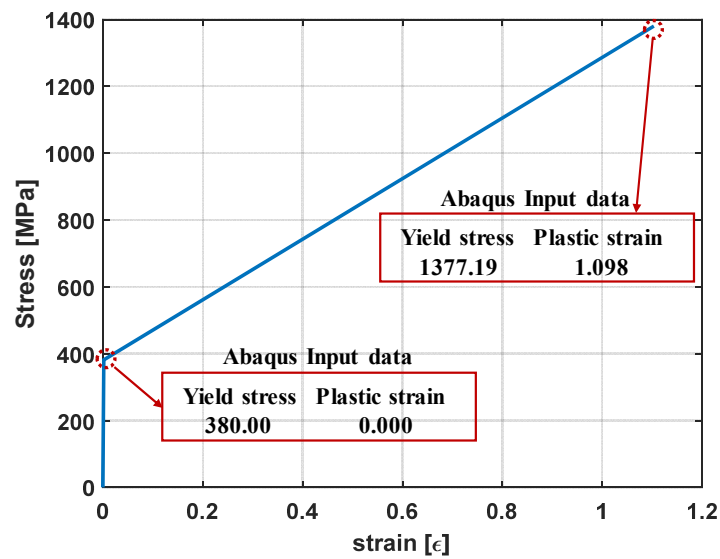


Figure 5. Material properties of the pipe.

Table 3. Material properties of the pipes.

Density [N/mm ³]	E [MPa]	Poisson's Ratio
7.85×10^{-9}	205,000	0.3

The finite element model of the piping using the beam element can simulate the test result well [22]. On the other hand, it is difficult to consider the activation of pipes caused by an excessive external force. Therefore, the finite element model of connection pipes was modeled using the shell element (S4R) of ABAQUS 6.14 to consider the effect of the elliptical deformation of pipes. Figure 6 shows a finite element model of the main steam piping. The total number of elements used is 17,168, and the number of nodes used is 17,052.

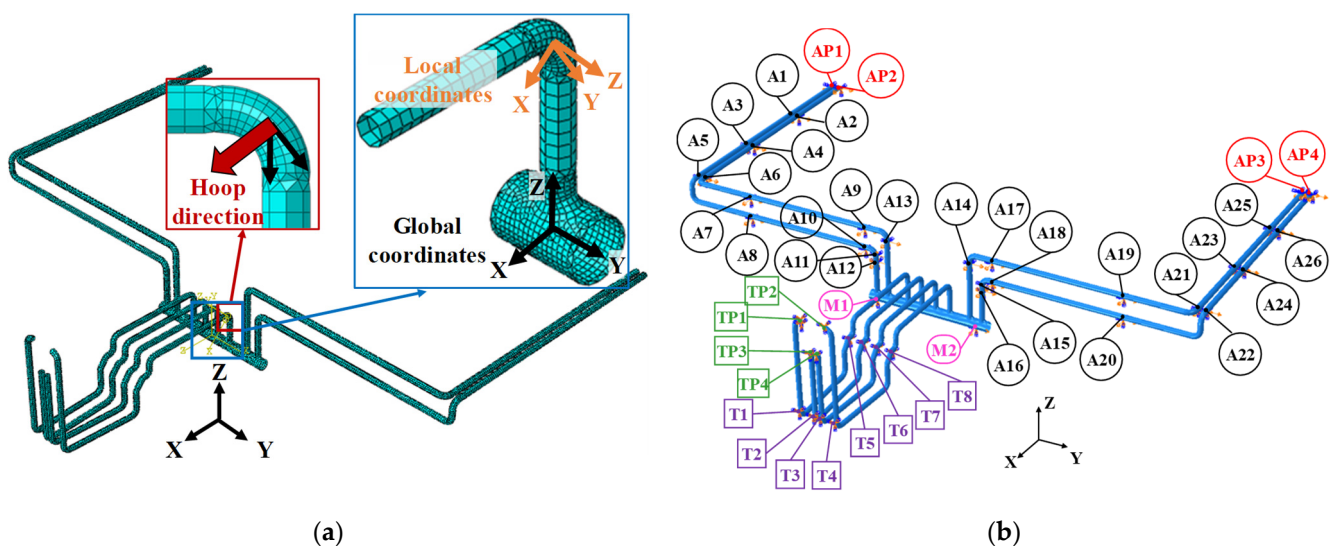


Figure 6. Cont.

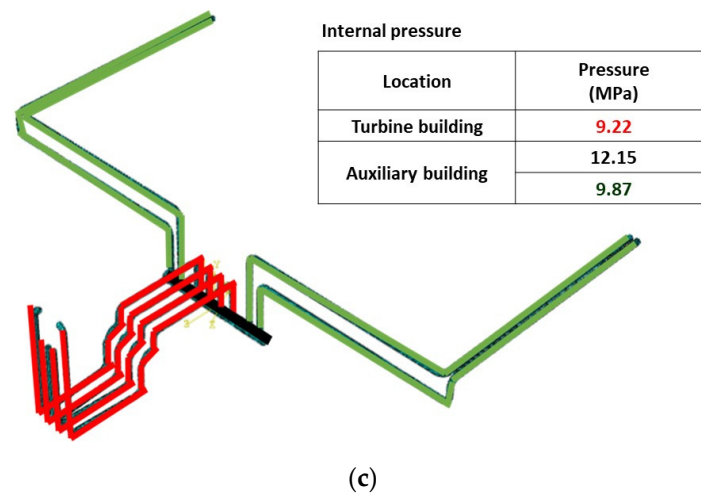


Figure 6. Finite element model of main steam piping: (a) Finite element model; (b) Boundary condition; (c) Internal pressure.

The finite element model of the pipe system is shown in Figure 6a. The boundary conditions were assumed, as shown in Table 4 and Figure 6b. The internal pressure of the pipe was calculated using Equation (1) [23]. The design temperature of the APR 1400 main steam piping was 299 °C [24], and the σ_{design} of Equation (1) was 115.9 MPa [25]. This was the same for SA-106 Gr.b pipe when the design temperature was 371 °C or less. Therefore, the internal pressure was calculated using Equation (1), as shown in Figure 6c. In Equation (1), I_p is internal design pressure; t , d and σ_{design} are the thickness, internal diameter, and design stress of the tube, respectively.

$$t = \frac{I_p d}{\sigma_{design} - 0.5 I_p} \quad (1)$$

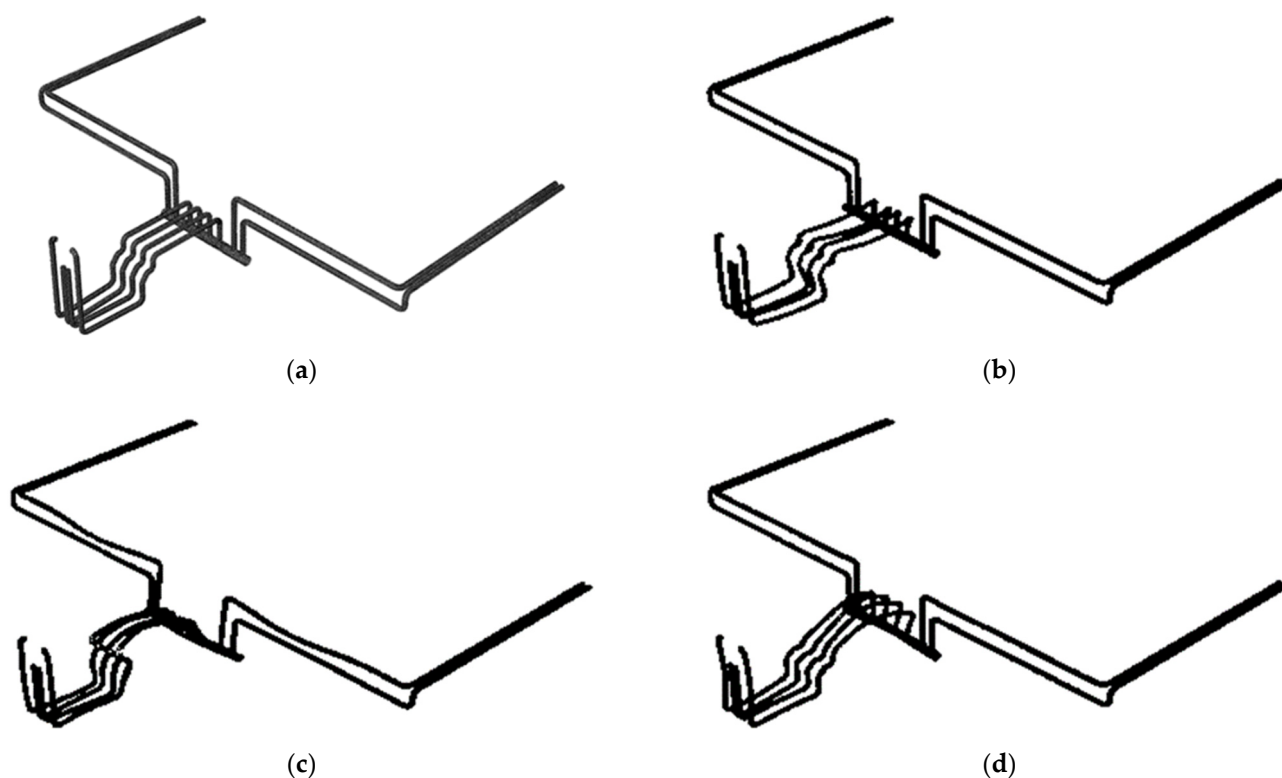
Table 4. Boundary conditions.

Support ID	Location		
	Building	Elevation [mm]	Constrained Directions
A1~A7, A9, A17, A19, A21~A26	auxiliary	42,589	X, Y
AP1~AP4	pedestal	42,589	X, Y, Z
A13, A14	auxiliary	41,067	X, Z
A8, A10, A18, A20	auxiliary	39,446	Y
A11, A15	auxiliary	38,417	Z
A12, A16	auxiliary	37,427	X
M1, M2	auxiliary	32,309	Y
TP1, TP2	pedestal	45,415	X, Y, Z
TP3, TP4	pedestal	41,300	X, Y, Z
T1~T4	turbine	32,181	X, Z
T5~T8	turbine	35,929	Y, Z

Table 5 and Figure 7 present the main mode and mode shapes of the main steam piping of the finite element model.

Table 5. Natural frequency and participation factors.

Model No.	Natural Frequency [Hz]	Participation Factors			Mass Participation Ratio		
		X	Y	Z	X	Y	Z
1	8.96	1.89800	0.08875	0.02998	1.00000	0.00219	0.00025
2	9.15	0.00343	0.98496	0.29788	0.00121	1.00000	0.09146
3	14.43	−0.00173	−0.67300	1.47700	0.00000	0.20792	1.00000

**Figure 7.** Mode shape of the piping system: (a) undeformed shape (b) 1st mode (8.69 Hz); (c) 2nd mode (9.15 Hz); (d) 3rd mode (14.43 Hz).

3. Results of Seismic Response Analysis

3.1. Maximum Stress and Strain

Nonlinear seismic response analysis was performed using the direct integration method while applying pressure inside the piping system and maintaining the stress caused by the internal pressure. Considering the reliability and convergence of the analysis, the input earthquake was used as the input displacement, and the stress and strain in the circumferential direction were obtained from the elbow crown, which is shown in Figure 6a. The input ground motion was considered for the horizontal bidirection. Table 6 lists the maximum relative displacement and MRD in each axial direction for the PGA size of the input ground motion. Here, MRD is the maximum value among the maximum relative displacement of the y - and x -directions. The MRD is at least 723 mm and a maximum of 1316 mm when the size of the PGA of the input earthquake is 1.0 g. Kim et al. [26] reported that the limit displacement under 2D horizontal input motion was 1120 mm for the lead rubber bearing (LRB) of the NPPs with an external diameter of 1520 mm; the total height of the rubber was 224 mm. Therefore, damage can occur when the size of the PGA is 1 g if the isolation system applied to the nuclear power plant is the LRB. In addition, damage to the isolation system was not included in the damage to the piping system. The nonlinear seismic response analysis showed that the elbow located at the boundary between seismic isolation and nonisolated structures was the most fatal factor, as shown in

Figure 6. Therefore, Figures 8 and 9 show the maximum stress and strain obtained from the elbow in Figure 6, respectively. Here, the seismic intensity is defined by the PGA and MRD.

Figures 8 and 9 show the maximum strain rate and stress, respectively. The average value of the maximum strain is 0.02696 when the PGA of the input ground motions is 1 g. The minimum and maximum values are 0.0135 and 0.0523, respectively. The average, minimum, and maximum stresses are 522.8 MPa, 424.6 MPa, and 612.29 MPa, respectively. The allowable stress was approximately 118 MPa at the design temperature of 343 °C or less in the ASME Boiler and Pressure Vessel Code [23], and the level D service limit was approximately 354 MPa because it is less than three times the allowable stress [25]. Therefore, in the case of earthquakes of 1 g or more, all input earthquakes exceeded the level D service limit, which is the design standard based on allowable stress. As shown in Table 7, a larger PGA indicates a greater standard deviation of the maximum strain and maximum stress.

Table 6. Maximum relative displacements between the isolation-non isolation building.

PGA Level	Relative Displacement [mm]														
	1 g			1.5 g			2 g			2.5 g			3 g		
	Direction		MRD	Direction		MRD	Direction		MRD	Direction		MRD	Direction		MRD
X	Y	X		Y	X		Y	X		Y	X		Y		
1	711	749	749	1376	1289	1376	2042	1838	2042	2704	2363	2704	3366	2888	3366
2	905	745	905	1595	1317	1595	2287	1888	2287	2996	2472	2996	3705	3056	3705
3	1268	638	1268	2132	1143	2132	2997	1648	2997	3859	2166	3859	4722	2684	4722
4	1042	696	1042	1770	1254	1770	2497	1812	2497	3234	2355	3234	3970	2898	3970
5	1266	677	1266	2064	1167	2064	2862	1656	2862	3672	2143	3672	4481	2652	4481
6	631	1046	1046	1027	1679	1679	1466	2315	2315	1983	2957	2957	2502	3612	3612
7	736	814	814	1269	1421	1421	1803	2032	2032	2328	2648	2648	2854	3263	3263
8	916	800	916	1506	1416	1506	2096	2037	2096	2691	2677	2691	3286	3318	3318
9	780	1009	1009	1427	1700	1700	2075	2392	2392	2726	3045	3045	3376	3698	3698
10	612	958	958	1098	1593	1593	1658	2230	2230	2219	2870	2870	2781	3510	3510
11	600	917	917	1064	1611	1611	1532	2305	2305	1990	3003	3003	2448	3701	3701
12	723	575	723	1409	1048	1409	2097	1525	2097	2778	2016	2778	3461	2508	3461
13	934	845	934	1514	1409	1514	2094	1978	2094	2656	2544	2656	3218	3109	3218
14	811	824	824	1319	1292	1319	1827	1766	1827	2343	2242	2343	2860	2733	2860
15	1098	726	1098	1835	1219	1835	2573	1779	2573	3305	2336	3305	4037	2893	4037
16	680	1081	1081	1259	1847	1847	1838	2614	2614	2423	3358	3358	3009	4102	4102
17	790	811	811	1369	1319	1369	1948	1827	1948	2535	2339	2535	3121	2851	3121
18	863	1045	1045	1416	1668	1668	1969	2291	2291	2520	2915	2915	3072	3540	3540
19	693	1079	1079	1171	1801	1801	1652	2563	2563	2125	3350	3350	2599	4138	4138
20	785	726	785	1271	1159	1271	1799	1669	1799	2405	2183	2405	3010	2697	3010
21	671	1065	1065	1113	1738	1738	1572	2411	2411	2051	3083	3083	2531	3756	3756
22	1179	524	1179	2110	900	2110	3042	1282	3042	3967	1660	3967	4892	2038	4892
23	607	1252	1252	1038	2103	2103	1468	2958	2958	1889	3841	3841	2310	4724	4724
24	654	766	766	1129	1383	1383	1607	2031	2031	2101	2680	2680	2595	3330	3330
25	1028	1169	1169	1654	1872	1872	2284	2575	2575	2902	3286	3286	3520	3998	3998
26	914	928	928	1587	1511	1587	2260	2094	2260	2948	2663	2948	3636	3237	3636
27	588	1316	1316	975	2111	2111	1362	2906	2906	1779	3699	3699	2210	4492	4492
28	1045	543	1045	1843	891	1843	2641	1305	2641	3442	1757	3442	4242	2211	4242
29	792	446	792	1510	873	1510	2243	1301	2243	2977	1737	2977	3711	2176	3711
30	846	635	846	1507	1171	1507	2192	1755	2192	2886	2314	2886	3580	2872	3580
Avg.	839	847	988	1445	1430	1675	2059	2026	2371	2681	2623	3071	3304	3223	3773

Table 7. Maximum responses according to the PGA level of input motions.

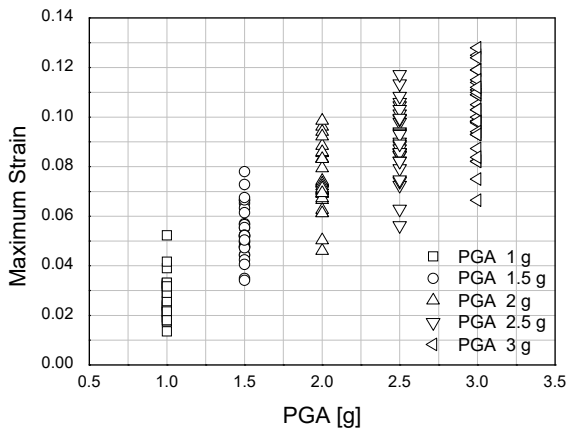
EQ	PGA Level									
	1 g		1.5 g		2 g		2.5 g		3 g	
	Max. ϵ	Max. σ [MPa]								
1	0.03	550.75	0.0664	711.48	0.0961	870.49	0.1134	991.02	0.1250	1110.00
2	0.0241	473.84	0.0476	603.62	0.0613	710.84	0.0725	827.94	0.0822	898.60
3	0.0390	564.21	0.0728	717.94	0.0986	943.65	0.1172	1039.39	0.1280	1160.00
4	0.0237	516.19	0.0495	653.65	0.0701	770.99	0.0844	878.13	0.0930	977.13
5	0.0328	532.61	0.0552	633.95	0.0733	772.27	0.0857	943.79	0.0984	1050.00
6	0.0235	528.60	0.0570	707.02	0.0834	896.99	0.0979	1026.97	0.1090	1160.00
7	0.0215	514.08	0.0444	575.31	0.0666	694.87	0.0854	845.66	0.0981	963.46
8	0.0272	545.96	0.0522	708.62	0.0708	893.28	0.0885	1045.78	0.1000	1190.00
9	0.0321	558.56	0.0566	716.42	0.0738	851.59	0.0847	1014.36	0.0931	1130.00
10	0.0214	534.42	0.0479	648.52	0.0706	790.21	0.0873	911.17	0.0977	1000.00
11	0.0179	500.82	0.0517	672.70	0.0832	862.86	0.1014	994.63	0.1140	1070.00
12	0.0326	525.93	0.0652	734.28	0.0884	909.07	0.1046	1058.89	0.1190	1260.00
13	0.0311	559.35	0.0554	658.96	0.0794	821.87	0.0941	949.25	0.1050	1040.00
14	0.0241	540.95	0.0523	682.40	0.0743	897.19	0.0899	1050.04	0.1030	1220.00
15	0.0280	497.82	0.0518	656.30	0.0690	772.71	0.0792	901.87	0.0873	1030.00
16	0.0231	476.43	0.0498	562.93	0.0732	725.00	0.0935	843.18	0.1090	946.92
17	0.0257	481.17	0.0522	641.04	0.0722	846.91	0.0857	989.36	0.0982	1140.00
18	0.0212	481.14	0.0442	613.06	0.0626	726.23	0.0740	826.34	0.0821	943.18
19	0.0175	424.61	0.0349	543.66	0.0461	735.27	0.0562	838.78	0.0664	947.06
20	0.0330	577.35	0.0632	741.93	0.0855	952.98	0.0992	1098.69	0.1110	1220.00
21	0.0190	485.54	0.0475	608.22	0.0673	731.17	0.0823	855.76	0.0941	970.46
22	0.0523	612.29	0.0779	857.98	0.0941	1040.00	0.1060	1177.69	0.1190	1350.00
23	0.0135	492.47	0.0424	638.73	0.0694	772.57	0.0931	951.04	0.1100	1070.00
24	0.0193	458.06	0.0341	539.53	0.0503	603.93	0.0629	680.28	0.0750	752.40
25	0.0215	520.17	0.0473	654.96	0.0712	786.30	0.0892	938.28	0.1030	1040.00
26	0.0291	447.91	0.0504	578.94	0.0693	785.87	0.0822	925.35	0.0929	1030.00
27	0.0180	502.63	0.0406	623.51	0.0612	731.84	0.0747	843.05	0.0838	959.56
28	0.0417	590.34	0.0666	784.37	0.0859	962.38	0.1032	1150.48	0.1150	1290.00
29	0.0332	593.92	0.0675	833.63	0.0922	1060.00	0.1084	1240.92	0.1240	1390.00
30	0.0317	595.84	0.0614	807.10	0.0831	982.21	0.0996	1133.77	0.112	1260.00
Avg.	0.0270	522.80	0.0535	670.36	0.0748	830.05	0.0899	965.73	0.1016	1085.63
Median	0.0249	523.05	0.0520	655.63	0.0727	806.04	0.0889	950.15	0.1015	1060.00
Min.	0.0135	424.61	0.0341	539.53	0.0461	603.93	0.0562	680.28	0.0664	752.40
Max.	0.0523	612.29	0.0779	857.98	0.0986	1060.00	0.1172	1240.92	0.1280	1390.00
Stdev.	0.0082	46.83	0.0105	81.41	0.0126	108.45	0.0140	124.17	0.0151	144.88

3.2. Damage Index

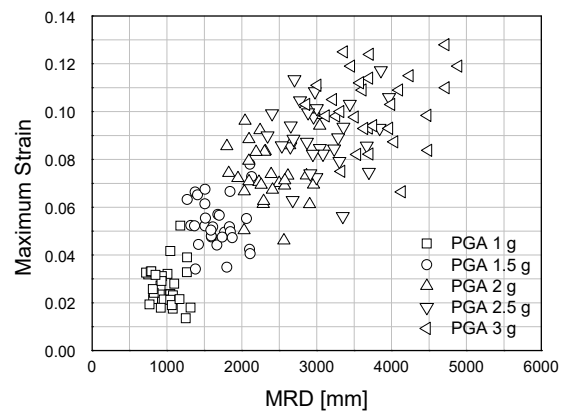
The actual damage to the pipe observed by the test is leakage-through cracks. Therefore, in this paper, leakage-through cracks, which can cause severe damage, such as loss of function of pipes and radiation leakage, were defined as failures. In general, damage to pipe elements under repeated dynamic loading, such as a seismic load, is fatigue failure [27,28]. In the case of pipes connecting the isolated structure and the general structure, large relative displacement can occur, even with a small number of repeated loadings, leading to failure. Therefore, low cycle fatigue should be considered a failure by the seismic load of the crossover piping system. The leakage-through cracks of pipes due to low cycle fatigue can be quantified using the damage index of Banon based on the relationship of stress-strain in Equation (2). The average damage index for the leakage-through crack of a three-inch SA106 SCH40 90° elbow was 35.25. Therefore, in this study, the 35.25 damage index was used as a failure criterion for the seismic fragility analysis of the main steam piping. In Equation (2), σ_y and ϵ_y are the yield stress and yield strain, respectively; ϵ_i and E_i

are the strain and dissipation energy of the i th cycle, respectively; c and d are the constants with corresponding values of 3.5 and 0.3 [9].

$$D = \sqrt{\left(\max\left(\frac{\varepsilon_i}{\varepsilon_y} - 1\right)\right)^2 + \left(\sum_{i=1}^N c \left(\frac{2E_i}{\sigma_y \varepsilon_y}\right)^d\right)^2} \quad (2)$$

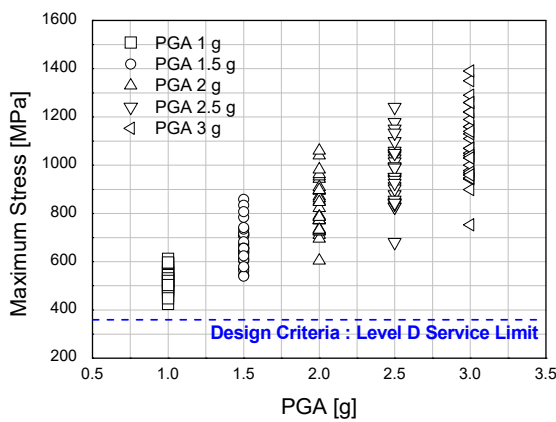


(a)

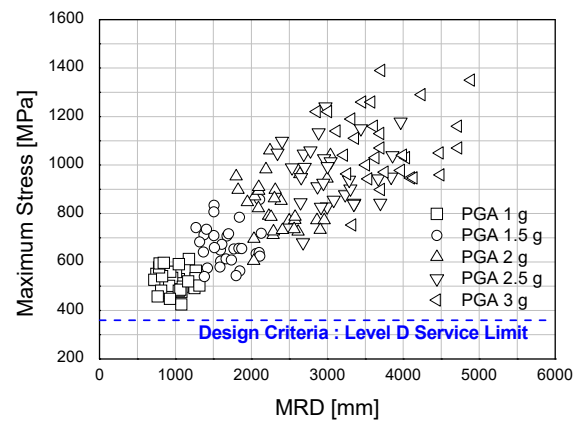


(b)

Figure 8. Maximum strain responses: (a) Maximum strain response according to the PGA; (b) Maximum strain response according to the MRD.



(a)



(b)

Figure 9. Maximum stress responses: (a) Maximum stress response according to the PGA; (b) Maximum stress response according to the MRD.

Figure 10 and Table 8 show the damage index calculated using Equation (2) from finite element analysis. In Figure 10a, when the PGA is 1.5 g or more, the average damage index was 31.61, and the median value was 30.62. The minimum and maximum values were 20.00 and 45.12, respectively. Therefore, if the size of the PGA in the input ground motion is more than 1.5 g, it can cause serious damage, such as radiation leakage. In addition, all damage indices exceeded the failure criteria when they were 3.0 g or more. In Figure 9, the maximum stress responses of the seismic response analysis exceeded all of the design criteria, Level D service limit, when the PGA of the input ground motion was 1 g. Therefore, there is a large difference between the design criteria of the pipe and the actual failure subjected to a seismic load.

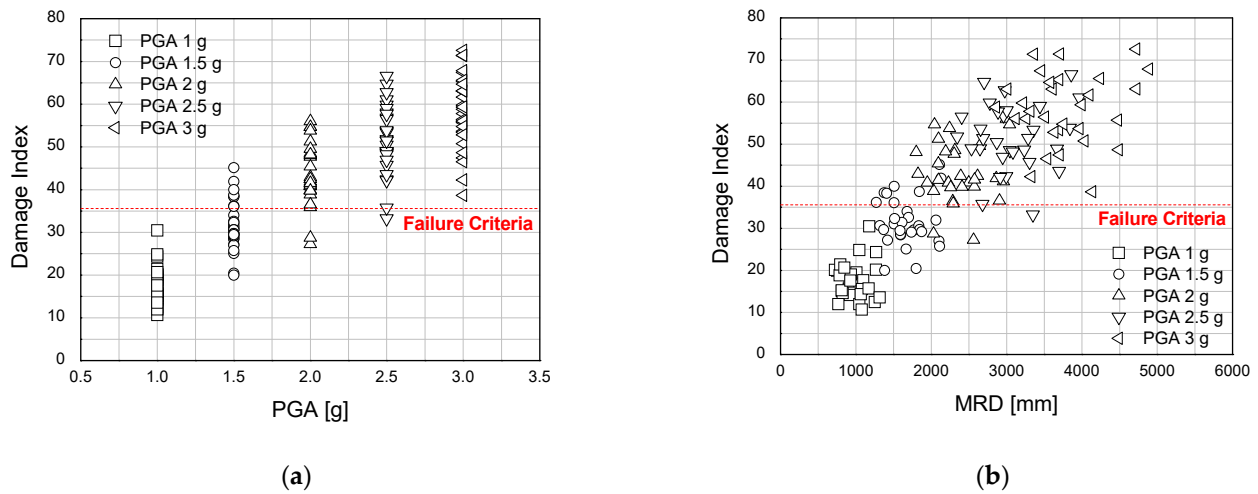


Figure 10. Damage indices: (a) Damage indices according to the PGA; (b) Damage indices according to the MRD.

Table 8. Damage indices of nonlinear analysis.

EQ	PGA Level				
	1 g	1.5 g	2 g	2.5 g	3 g
1	19.94	38.43	54.67	64.72	71.35
2	15.68	28.42	36.41	42.32	47.44
3	24.35	41.91	56.04	66.55	72.57
4	15.10	29.61	40.86	48.65	53.67
5	20.15	31.94	41.91	48.89	55.71
6	16.90	34.01	48.55	56.76	63.05
7	15.11	27.19	38.84	48.94	56.08
8	17.81	31.02	41.52	51.40	57.81
9	19.49	32.55	42.47	48.53	53.42
10	14.69	28.51	40.81	50.43	56.41
11	14.17	31.40	47.71	58.01	65.31
12	20.13	38.32	51.27	59.81	67.41
13	18.98	32.31	45.41	53.63	59.80
14	14.58	30.64	42.96	51.75	58.80
15	17.63	30.59	39.89	45.74	50.78
16	15.54	29.74	42.44	53.35	61.69
17	15.29	29.69	40.85	48.98	56.05
18	11.98	25.07	35.88	42.12	46.54
19	10.68	20.44	27.28	33.24	38.66
20	18.82	36.14	48.12	56.47	63.07
21	14.32	29.07	39.83	48.19	54.75
22	30.44	45.12	54.67	61.05	67.83
23	12.50	27.00	41.15	53.80	63.10
24	12.01	20.00	28.75	35.74	42.27
25	15.71	29.21	41.54	51.43	59.33
26	17.58	29.47	39.75	46.95	52.80
27	13.55	25.74	36.55	43.59	48.66
28	24.86	38.72	49.55	59.02	65.56
29	21.45	39.99	53.82	62.73	71.43
30	20.65	36.08	48.26	57.66	64.67
Avg.	17.34	31.61	43.26	51.68	58.20
Median	16.31	30.62	41.73	51.42	58.31
Max.	30.44	45.12	56.04	66.55	72.57
Min.	10.68	20.00	27.28	33.24	38.66
Stdev.	4.29	5.80	7.04	7.90	8.52

As shown in Figure 10a, when the PGA is set to the seismic intensity, 30 responses were obtained at each PGA level. A higher PGA means a greater standard deviation between the response and damage index (Table 8). This is similar to the case of maximum stress and maximum strain. Artificial earthquakes for seismic safety evaluation are mostly prepared based on acceleration. Therefore, most displacements from artificial earthquakes with the same PGA size are different. In particular, as shown in this study, the sizes of the relative displacement of isolated structures and nonisolated structures were determined by the characteristics of the isolation system by applying it to the lower part of the structure were greatly different. Therefore, when MRD is used as the seismic intensity, the maximum response is dispersed according to the size of MRD of each input ground motion, as shown in Figure 10b. A larger PGA indicates a broader distribution of the MRD and a higher damage index. In particular, even if the size of the PGA is small, the size of the MRD and the value of the damage index may be larger.

To design an isolation system for NPP, it is necessary to calculate the probability of failure of the crossover piping system. The seismic fragility curve of the crossover piping system should consider MRD, the one-way maximum relative displacement acting on the isolation system. The fragility curve of pipes with the PGA as the seismic intensity could not propose acceptable displacement and the probability of failure for the design of the isolation system. On the other hand, for the probabilistic safety assessment (PSA) of nuclear power plants, it is necessary to perform seismic fragility analysis according to the PGA. Therefore, this paper prepared seismic fragility curves for the main steam piping of an isolated APR1400 NPP with the PGA and MRD as the seismic intensity. The probability of failure was 5% when the PGA was 1.25 g or the MRD was 1156 mm, and 50% when the PGA was 1.65 g and the MRD was 1800 mm.

4. Seismic Fragility Analysis

The seismic fragility curve is in the form of a lognormal distribution function [29]. The median value and the logarithmic standard deviation are two important variables in the seismic fragility comprising the bivariate lognormal distribution. In general, the probability of failure of a structure is defined when an arbitrary seismic load a is applied, as shown in Equation (3). In Equation (3), p_R is the probability density function of the response, and p_C is the probability density function of the internal force.

$$P_f(a) = \int_0^{\infty} p_R(a, x_R) \left[\int_0^{x_R} p_C(x) dx \right] dx_R \quad (3)$$

Equation (3) can be expressed as Equation (4), considering the internal force and uncertainty in response. Here, C_m is the median internal force; R_m is the median structural response; $\Phi(\cdot)$ is the cumulative probability distribution of the standard normal distribution function; β_C is the logarithmic standard deviation of the compound probability variable.

$$P_f(a) = 1 - \Phi \left[\frac{\ln C_m - \ln R_m(a)}{\beta_C} \right] \quad (4)$$

β_C in Equation (4), can be expressed as the square root of the sum of squares of the logarithmic standard deviation β_R of the probability variable considering randomness and the algebraic standard deviation β_U , which means uncertainty, as shown in Equation (5).

$$\beta_C = \sqrt{\beta_R^2 + \beta_U^2} \quad (5)$$

In this paper, 0.033 was used as the logarithmic standard deviation β_U of the damage index obtained from the element test and finite element analysis of a carbon steel plate elbow conducted in a previous study [9]. The logarithmic standard deviation β_R of randomness is the randomness of the response induced by the results of nonlinear seismic response analysis. The input ground motion showed less variability because the seismic wave

suitable for the design response spectrum was input. It would be reasonable to use the seismic wave suitable for the design response spectrum to review the structure's performance. In addition, the coefficient of variation was applied with the logarithmic standard deviation because it was assumed that the distribution of responses follows the lognormal distribution. A seismic fragility curve was prepared using the failure probability calculated using Equation (3), as shown in Figure 11.

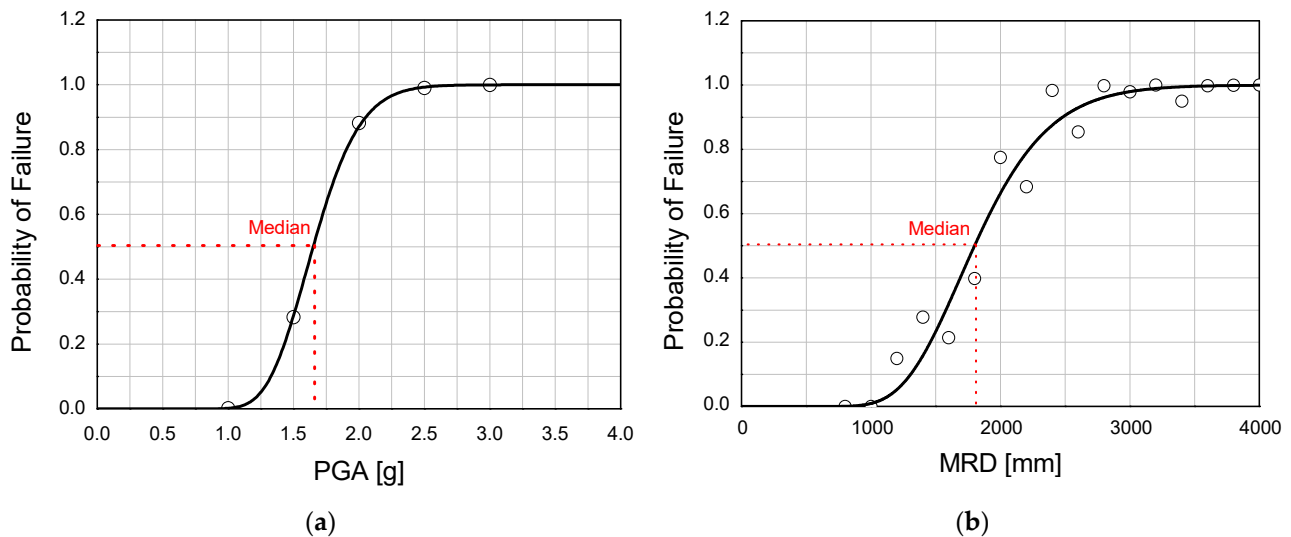


Figure 11. Fragility curves for main steam piping of isolated NPP: (a) PGA-based fragility curve; (b) MRD-based fragility curve.

Figure 11a is a seismic fragility curve prepared using the PGA as a seismic intensity. The PGA, which has a 5% probability of failure, is 1.25 g, and the median is 1.65 g. It is necessary to consider the probability of pipe damage to the relative displacement when designing an isolation system for an NPP with a pipe connecting the isolated-non isolated section. The relative displacement of the isolation system corresponding to the probability of failure of the pipe was not identified when the PGA was set as seismic intensity, as shown in Figure 11a. When MRD is used as the seismic intensity, the damage index is dispersed, as shown in Figure 10b. Therefore, in this study, the probability of failure was calculated by dividing the size of MRD per 200 mm intervals. Figure 11b shows the fragility curve prepared using MRD as the seismic intensity. The MRD with a 5% probability of failure is 1156 mm, and the median of the seismic fragility curve is 1800 mm. Table 9 lists the probability of failure in Figure 11.

Table 9. Seismic performance of main steam piping of isolated NPP.

Probability of Failure	Seismic Intensity	
	PGA [g]	MRD [mm]
5%	1.25	1156
50%	1.65	1800

5. Summaries and Conclusions

This paper performed seismic fragility analysis targeting the main steam piping and a crossover piping system of a Korean standard nuclear power plant with an isolation system. The fragility criteria for seismic fragility analysis were defined as leakage-through cracks that can cause serious damage, such as loss of function of pipes and radiation leakage. A nonlinear seismic response analysis was performed by adjusting the acceleration of 30 sets of horizontal bidirectional artificial earthquakes. As a result, the most dangerous component in the crossover piping system is the elbow.

In the case of the main steam piping of an isolated APR1400 NPP, which is assumed to support conditions. When the PGA of the input ground motion is 1 g, the maximum stress response at the crown of the pipe elbow exceeds the Level D service load. However, no leakage-through cracks occur. On the other hand, if the level of the PGA in the input ground motion is more than 1.5 g, it can exceed the damage index for failure, which can cause serious damage, such as radiation leakage. Therefore, for accurate seismic fragility analysis, the damage index for leakage-through cracks, which is an actual failure, was used as the fragility criterion.

Results of nonlinear seismic response analysis showed that a higher PGA level indicated a higher standard deviation of the maximum stress, maximum strain, MRD, and damage index. Since the input ground motion was prepared based on the PGA, when the maximum response values of the nonlinear seismic response analysis are arranged according to each level of the PGA, one set of maximum response values is arranged in the PGA of a specific level. However, when MRD is used as the seismic intensity, the maximum responses are dispersed. Additionally, even if the size of the PGA is small, the size of the MRD and the damage index can be larger. The same trend appears in the case of the damage index.

The seismic fragility curve of the crossover piping system using the PGA and MRD may be a parameter that can be considered when designing an isolation system. In this paper, seismic fragility analysis was performed using the seismic intensity of PGA and MRD. When the PGA is 1.25 g or the MRD is 1156 mm, the failure probability is 5%. When the PGA is 1.65 g and the MRD is 1800 mm, the damage probability is 50%.

As a further study, research on adjustable joints and flexible pipes is in progress to reduce the damage to the pipe passing through the interface of the seismic isolation system.

Author Contributions: Conceptualization, S.E.; Formal analysis, S.-W.K. and D.-W.Y.; Investigation, D.H.; Writing—original draft, B.-G.J.; Writing—review & editing, S.E. All authors have read and agreed to the published version of the manuscript.

Funding: This research was supported by the Korea Agency for Infrastructure Technology Advancement (KAIA) grant funded by the Ministry of Land, Infrastructure and Transport of Korean government (No. 22CTAP-C164263-02).

Institutional Review Board Statement: Not applicable.

Informed Consent Statement: Not applicable.

Conflicts of Interest: The authors declare no conflict of interest.

References

1. Jang, K.S.; Chnag, H.P.; Lee, H.P. Influence evaluation of the multi-lead rubber bearing due to the compressive stress for nuclear power plant. *J. Korean Soc. Adv. Compos. Struct.* **2016**, *7*, 55–64. [[CrossRef](#)]
2. Kammerer, A.M.; Whittaker, A.S.; Constantinou, M.C. *Technical Considerations for Seismic Isolation of Nuclear Facilities (NUREG/CR-7253)*; U.S. Nuclear Regulatory Commission: Washington, DC, USA, 2019.
3. Vailati, M.; Monti, G.; Bianco, V. Integrated solution-base isolation and repositioning-for the seismic rehabilitation of a preserved strategic building. *Buildings* **2021**, *11*, 164. [[CrossRef](#)]
4. Monti, G.; Vailati, M.; Marnetto, R. Base Isolation and Translation of a Strategic Building Under a Preservation Order. In *Earthquakes and Their Impact on Society*; Springer: Cham, Switzerland, 2016; pp. 433–447.
5. Cheung, J.H.; Gae, M.S.; Seo, Y.D.; Choi, H.S.; Kim, M.K. Seismic capacity test of nuclear piping system using multi-platform shake table. *J. Earthq. Eng. Soc. Korea* **2013**, *17*, 21–31. [[CrossRef](#)]
6. Hahm, D.G.; Park, J.H.; Choi, I.K. Seismic performance evaluation of piping system crossing the isolation interface in seismically isolated NPP. *J. Earthq. Eng. Soc. Korea* **2014**, *18*, 141–150. [[CrossRef](#)]
7. Jeon, B.G.; Kim, S.W.; Choi, H.S.; Park, D.U.; Kim, N.S. A failure estimation method of steel pipe elbows under in-plane cyclic loading. *Nucl. Eng. Technol.* **2017**, *49*, 245–253. [[CrossRef](#)]
8. Kim, S.W.; Chang, S.J.; Park, D.U.; Jeon, B.G. Failure criteria of a carbon steel pipe elbow for low-cycle fatigue using the damage index. *Thin-Walled Struct.* **2020**, *153*, 106800. [[CrossRef](#)]
9. Kim, S.W.; Jeon, B.G.; Hahm, D.G.; Kim, M.K. Seismic fragility evaluation of the base-isolated nuclear power plant piping system using the failure criterion based on stress-strain. *Nucl. Eng. Technol.* **2019**, *51*, 561–572. [[CrossRef](#)]

10. Xu, J.; DeGrassi, G.; Chokshi, N. A NRC-BNL benchmark evaluation of seismic analysis methods for non-classically damped coupled systems. *Nucl. Eng. Des.* **2004**, *228*, 345–366. [[CrossRef](#)]
11. Eem, S.H.; Choi, I.K.; Cha, S.L.; Kwag, S.Y. Seismic response correlation coefficient for the structures, systems and components of the Korean nuclear power plant for seismic probabilistic safety assessment. *Ann. Nucl. Energy* **2021**, *150*, 107759. [[CrossRef](#)]
12. Eem, S.H. Seismic Fragility Assessment of Isolated Structures Based on Stochastic Response Database. Ph. D. Thesis, Korean Advanced Institute for Science and Technology, Daejeon, Korea, 2014.
13. Eem, S.H.; Jung, H.J. Seismic response distribution estimation for isolated structures using stochastic response database. *Earthq. Struct.* **2015**, *9*, 937–956. [[CrossRef](#)]
14. Eem, S.H.; Jung, H.J. Seismic fragility assessment of isolated structures by using stochastic response database. *Earthq. Struct.* **2018**, *14*, 389–398.
15. American Society of Civil Engineers. *Minimum Design Loads for Buildings and Other Structures (ASCE/SEI 7-05)*; American Society of Civil Engineers: New York, NY, USA, 2005.
16. Federal Emergency Management Agency. *NEHRP Recommended Provisions: Design Examples (FEMA-451)*; Federal Emergency Management Agency: Washington, DC, USA, 2006.
17. United States Nuclear Regulatory Commission. *Design Response Spectra for Seismic Design of Nuclear Power Plants (Regulatory Guide 1.60)*; United States Nuclear Regulatory Commission: Washington, DC, USA, 2014.
18. American Society of Civil Engineers. *Seismic Analysis of Safety-Related Nuclear Structures (ASCE/SEI 4-16)*; American Society of Civil Engineers: New York, NY, USA, 2016.
19. Ohno, S. Strong-motion characteristics during the 2011 Tohoku earthquake. *J. Jpn. Landslide Soc.* **2013**, *50*, 75–82. [[CrossRef](#)]
20. The American Society of Mechanical Engineers. *Welded and Seamless Wrought Steel Pipe (ASME B36.10M)*; The American Society of Mechanical Engineers: New York, NY, USA, 2015.
21. Jeon, B.G.; Kim, S.W.; Yun, D.W.; Hahm, D.G. A Quantitative Limit State of the Carbon Steel Pipe Tee in the Nuclear Power Plants Under In-Plane Cyclic Loading. In Proceedings of the 25th International Conference in Structural Mechanics in Reactor Technology (SMiRT-25), Charlotte, NC, USA, 4–9 August 2019.
22. Kwag, S.Y.; Eem, S.H.; Kwak, J.S.; Oh, J.H. Evaluation model of seismic response behavior and performance of nuclear plant piping systems. *J. Korean Soc. Adv. Compos. Struct.* **2020**, *11*, 54–62. [[CrossRef](#)]
23. American Society of Mechanical Engineers. Section III, Rules for Construction of Nuclear Facility Components. In *ASME Boiler and Pressure Vessel Code*; American Society of Mechanical Engineers: New York, NY, USA, 2015.
24. Korea Electric Power Corporation Engineering & Construction. *SKN 3 & 4 Safety Related-Plant Manual-Main Stem System (MS)*; Korea Electric Power Corporation Engineering & Construction: Yongin, Korea, 2011.
25. American Society of Mechanical Engineers. Section II, Part D, Properties (Customary). In *ASME Boiler and Pressure Vessel Code*; American Society of Mechanical Engineers: New York, NY, USA, 2015.
26. Kim, J.H.; Kim, M.K.; Choi, I.K. Experimental study on seismic behavior of lead-rubber bearing considering bi-directional horizontal input motions. *Eng. Struct.* **2019**, *198*, 109529. [[CrossRef](#)]
27. Zhang, T.; Brust, F.W.; Willkowsky, G.; Shim, D.J.; Nie, J.; Hofmayer, C.H.; Ali, S.A. Analysis of JNES Seismic Tests on Degraded Piping. In Proceedings of the ASME 2010 Pressure Vessels & Piping Division/K-PVP Conference, Washington, DC, USA, 18–22 July 2010.
28. Electric Power Research Institute. *Piping and Fitting Dynamic Reliability Program (EPRI TR-102792-V1 through V5)*; Electric Power Research Institute: Palo Alto, CA, USA, 1994.
29. Shinozuka, M.; Feng, M.Q.; Kim, H.K.; Kim, S.H. Nonlinear static procedure for fragility curve development. *J. Eng. Mech.* **2000**, *126*, 1287–1296. [[CrossRef](#)]